CHEMISTRY
A EUROPEAN JOURNAL

ChemPubSoc
Europe

DOI: 10.1002/chem.201301081

A Designed 5-Fluorouracil-Based Bridged Silsesquioxane as an Autonomous Acid-Triggered Drug-Delivery System

Simon Giret,[a] Christophe Théron,[a] Audrey Gallud,[b] Marie Maynadier,[b] Magali Gary-Bobo,[b] Marcel Garcia,[b] Michel Wong Chi Man,[a] and Carole Carcel*[a]

Abstract: Two new prodrugs, bearing two and three 5-fluorouracil (5-FU) units, respectively, have been synthesized and were shown to efficiently treat human breast cancer cells. In addition to 5-FU, they were intended to form complexes through H-bonds to an organo-bridged silane prior to hydrolysis-condensation through sol–gel processes to construct acid-responsive bridged silsesquioxanes (BS). Whereas 5-FU itself and the prodrug bearing two 5-FU units completely leached out from the corresponding materials, the prodrug bearing three 5-FU units was successfully maintained in the resulting BS. Solid-state NMR (^{29}Si and ^{13}C) spectroscopy show that the organic fragments of the organo-bridged silane are retained in the hybrid through covalent bonding and the ^{1}H NMR spectroscopic analysis provides evidence for the hydrogen-bonding interactions between the prodrug bearing three 5-FU units and the triazine-based hybrid matrix. The complex in the BS is not affected under neutral medium and operates under acidic conditions even under pH as high as 5 to deliver the drug as demonstrated by HPLC analysis and confirmed by FTIR and ^{13}C NMR spectroscopic studies. Such functional BS are promising materials as carriers to avoid the side effects of the anticancer drug 5-FU thanks to a controlled and targeted drug delivery.

Keywords: cancer · drug delivery · drug design · hydrogen bonding · sol–gel processes

Introduction

In the past few decades, several kinds of nanomaterials have been developed for application in biological and medical fields, such as sensors, cell markers, and drug-delivery systems.[1] The latter is particularly one of the most exciting challenges to take up and it is now established that well-designed drug carriers with controlled delivery can overcome some issues of conventional therapy and enhance the therapeutic performance of a given drug. For a maximum therapeutic efficiency, an optimal amount of the agent must be delivered without premature release to the targeted cell. This would avoid the use of any excess of the drug, which would reduce general toxicity and would cause minimal side effects. Several approaches have since been developed to deliver antimicrobial or therapeutic substances to the target site among which mesoporous silica nanoparticles (MSN)[1e,2] appear as one of the most promising strategies that is being adopted by many researchers. Indeed, MSN have superior features compared with organic polymers exhibiting highly ordered porous structure, tunable pore size, pore volume, and high surface areas, which can be exploited as reservoirs for active molecules. Moreover, silica provides mechanical and chemical stabilities, efficient protection for the payloads as well as biocompatibility and is non-toxic when in the amorphous state.[3] These MSNs are mostly being developed for medical applications,[1g,4] and a main objective is to achieve specifically drug administering to target cells. Quite recently, striking achievements have been highlighted with newly synthesized stimuli-responsive MSN nanomachines to deliver cargo molecules. To obtain efficient nanosystems, MSNs have been functionalized with organic groups that can act as caps, gatekeepers, valves, and so on,[1g,4a–c], which can be operated under an appropriate stimuli (pH, redox potential, magnetic, etc.) to deliver the cargo molecules after pore openings.[5]

Since its introduction in the last two decades, bridged silsesquioxanes (BS)[6] have fascinated scientists because they are hybrid materials with a high content of organic groups linked regularly to the silica matrix and can thus combine both the properties of the latter with those of the organic components.[7] Owing to the wide variety of organics and to their intrinsic properties that can be introduced in BS, our group has been exploring their uses in several application fields such as catalysis,[8] solid-state lighting and luminescent

[a] S. Giret, C. Théron, Dr. M. Wong Chi Man, Dr. C. Carcel
Laboratory Architectures Moléculaires et Matériaux Nanostructurés
Institut Charles Gerhardt Montpellier
(UMR 5253 CNRS-UM2-ENSCM-UM1)
ENSCM, 8 rue de l'école normale
34296 Montpellier (France)
E-mail: carole.carcel@enscm.fr

[b] A. Gallud, Dr. M. Maynadier, Dr. M. Gary-Bobo, Dr. M. Garcia
Institut des Biomolécules Max Mousseron
UMR 5247 CNRS, Université Montpellier 1
Université Montpellier 2, ENSCM
Faculté de Pharmacie, 15 Avenue Charles Flahault
34093 Montpellier Cedex 05 (France)

Supporting information for this article is available on the WWW under http://dx.doi.org/10.1002/chem.201301081.

solar concentrators[9] or for selective ion uptake.[10] In BS, porosity can be created, for example, by cleavage of the covalently bonded sacrificial organics in the silica matrix[11] or by using surfactants to create ordered mesopores. In the latter case, periodic mesoporous organosilicates (PMOs)[12] are obtained in which either the organics are located in the walls from which they can be randomly dispersed[6b,7a] or well-arranged; in the latter case, a hierarchical crystalline hybrid silica is formed.[13] A recent review gives a compilation of different applications of PMO's, for example, as catalysts and adsorbents for which the high surface area and porosity are the bare essentials.[14] Consequently, like MSN, PMOs have also been used as drug-delivery systems[15] and it was shown that the morphology of the material (hollow spheres vs. solid spheres)[15a] as well as the organic functions inside the walls (compared with functionalized MSN)[15b] could improve or affect their drug-release properties. To date, the use of PMOs in this field is still in its infancy because they are not easy to synthesize in a pure state without avoiding the use of mixing the organobridge precursor with other alkoxysilane precursors such as tetramethylorthosilicate (TMOS) and tetraethylorthosilicate (TEOS),particularly when the bridging organic unit is voluminous.[16]

Herein, we used another concept to design new BS-based drug carriers in which high porosity and high surface area are not required features. The BS is synthesized with the corresponding bridge organosilane precursor in the presence of a non-silylated molecule, which is held by weak H-bonding interactions in the resulting BS. This molecule plays the double role of the templating agent and the drug itself. The drug release (in this case the templating molecule) can be achieved by applying an acidic pH that cleaves the H-bonds.

We recently reported a new family of BS synthesized from monosilylated complementary base-pair derivatives in which the two organic units are linked together (molecular recognition) by H-bonding to form the bridging unit.[17] Solid-state ^{1}H NMR spectroscopic investigations revealed the preservation of the molecular recognition sites[18] and the preserved H-bonds are even shown to play an important role in the nanostructuring of a ureidopyrimidinone-based BS.[19] These original BS are prone to applications and thus a molecular-imprinted BS[20] and more recently a pH-sensitive BS have been reported.[21] The latter was designed from a bis-silylated triazine derivative **P1** (Figure 1) with a **DAD** (donor–acceptor–donor) pattern H-bonded with cyanuric acid (CA) bearing the complementary **ADA** (acceptor–donor–acceptor) patterns (9 H bonds).

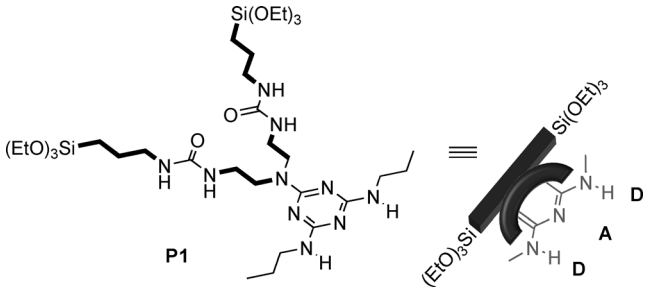

Figure 1. Structure of precursor **P1**.

It was shown that the templating CA molecule could completely be removed from the material upon acid treatment and interestingly even under a mild acidic medium (pH 5.5). It is known that pH values vary significantly in different tissues and cellular compartments. While it is close to neutral in blood and normal tissues (pH 7.4), it is lightly acidic in tumoral tissues (pH 6.8) and more acidic in endosomal (pH 6–5.5) and lysosomal (pH 5.0–4.5) compartments.[22] We thus decided to investigate this pH-sensitive BS and see whether it is likely to be developed as a drug platform for controlled drug-delivery. We chose 5-fluorouracil (5-FU) as the drug candidate as it bears an adequate **ADA** pattern, which makes it liable to associate with the **DAD** pattern of **P1** (Figure 2). Moreover, it is commonly used as an anticancer

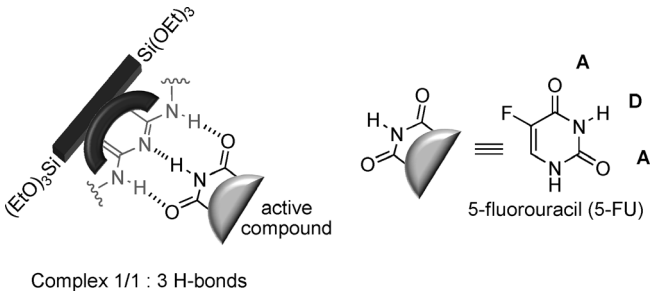

Figure 2. Schematic representation of the H-bonding interaction between **P1** and 5-FU.

drug in the clinical treatment of several solid cancers, such as breast, colorectal, liver, and brain cancer. Due to its high rate of metabolism in the body, a high concentration of 5-FU is needed to improve its therapeutic effect. A continuous administration of 5-FU is thus required, which represents a serious drawback since a concentration above a certain limit produces severe side effects. To overcome this issue, controlled and targeted release of 5-FU is needed. Thus, the strategy to construct a BS holding a 5-FU unit by molecular recognition patterns is quite appealing because a direct and controlled release of the drug in the cell will be self-triggered by the acidic pockets of the cells.

To evaluate the role of the amount of H-bonds on the stability of this new system and consequently on the release rate of the drug under neutral and acidic conditions, we considered two new compounds (**2** and **3**), with two and three 5-FU units, respectively (Figure 3) for which we also studied the in vitro toxicity towards human breast cancer cells.

Results and Discussion

The objective of this work was to make use of a bridged silsesquioxane BS that can hold 5-FU at neutral pH (like in

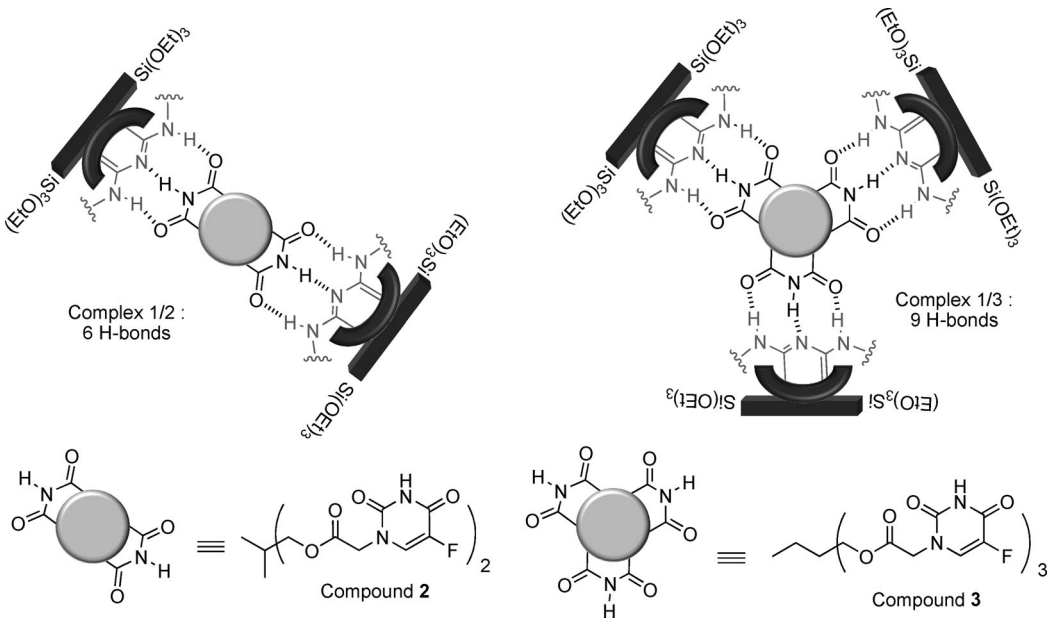

Figure 3. Structures of new 5-FU-based prodrugs **2** and **3** and their H-bonding association with **P1**.

blood medium) to create a new type of carriers with no premature release of the drug and to demonstrate that its direct and controlled release can be triggered by the acidic pH close to those found in the acidic compartments of cells.

Syntheses and studies of 2 and 3: In addition to 5-FU, which is used as drug model, two new 5-FU prodrugs (**2** and **3**) with two and three 5-FU units, respectively, linked through an ester function to an alkyl core were synthesized (Figure 3). These linkers can be cleaved chemically or enzymatically[23,24] to generate 5-FU and/or 5-fluorouracil-acetic acid (5-FUA also referred to as compound **1** in this work) whose biological activities are known.[25]

Syntheses: Compounds **2** and **3** were prepared as described in Scheme 1. Compound **1** (5-FUA) was obtained according to a known procedure[23a] by treating 5-FU with chloroacetic acid in alkaline solution at 60 °C. Adding an excess of thionyl chloride to compound **1** led to the formation of the corresponding acyl chloride. The latter was then treated with 2,2-dimethylpropane-1,3-diol and with 1,1,1-tri(hydroxymethyl)-propane to afford **2** and **3**, respectively.

*Investigations on the association of 5-FU and compounds **2** and **3** with **P1***: We first investigated the association feasibility between 5-FU and the BS precursor **P1** by performing liquid ^{1}H NMR spectroscopic studies in [D$_6$]DMSO (Figure 4). In the ^{1}H NMR spectrum of 5-FU, it was not possible to distinguish between the two protons, H–N3 and H–N1, because they exist as a single broad peak at $\delta =$ 11.1 ppm. On the addition of one equivalent of **P1**, these two H separated into two distinct and well-resolved peaks at $\delta = 10.9$ and 11.8 ppm. This implies that the proton of H–N3 is involved in the H-bonding process with the **DAD** face of

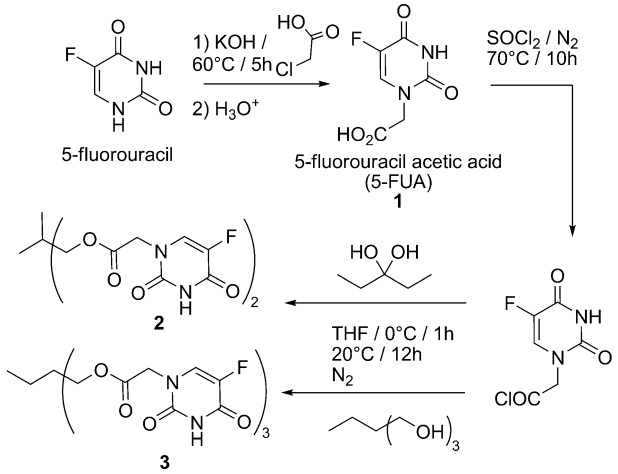

Scheme 1. Synthesis of compounds **2** and **3**.

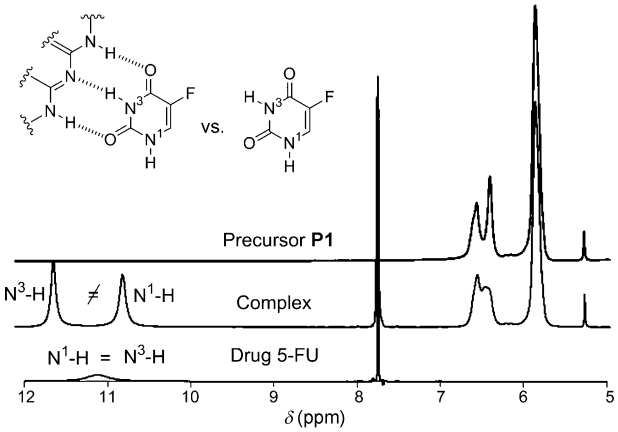

Figure 4. Liquid ^{1}H NMR spectrum in [D$_6$]DMSO of 5-FU, **P1**, and complex 5-FU/**P1** (1:1).

P1, which confirms the complex formation between **P1** and 5-FU.

Similarly to 5-FU, the N3 proton of 5-FU units in **2** and **3** was used to probe the H-bonding interactions. As shown in Figure 5a, the probe proton of **2** appears as a sharp peak at $\delta = 12.0$ ppm. In this case, since **2** bears two 5-FU units, a 1/2 molar equivalent of **P1** was used to form the complex (Figure 3). Following the addition of **P1**, no significant shift was observed but this peak broadens and the chemical shift ranges from $\delta = 11.7$ to 12.3 ppm. Similar observations were made in the spectrum of **3** (Figure 5b), which exhibits a sharp singlet at $\delta = 12$ ppm and broadens (from $\delta = 11.5$ to 12.5 ppm) on addition of 1/3 molar equivalent of **P1**. As in the case of 5-FU this change can be attributed to H-bonding formation of the H–N3 of the 5-FU prodrugs with the silylated precursor **P1**.

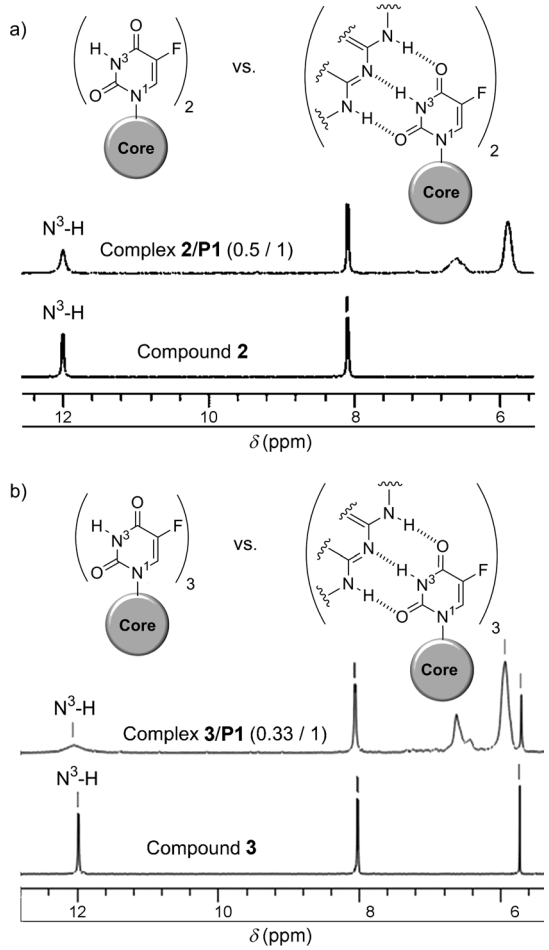

Figure 5. Liquid ^{1}H NMR spectra of complex between a) compound **2** and **P1**, and b) compound **3** and **P1** in [D_6]DMSO.

In vitro toxicity: The biological potential of the newly synthesized prodrugs of 5-FU (**2** and **3**) was established by a cytotoxic assay on human breast cancer cells (MCF-7). For this, cell cultures were treated by increasing doses of **2** and **3** (from 5 to 50 μM). For comparison, cell cultures were also treated in the same conditions with compound **1** and 5-FU. All compounds induced a decrease in the cell number compared to control cells, which are treated with equivalent volumes of the vehicle (DMSO) (Figure 6a). This effect was confirmed by a MTT assay, which demonstrated that the four molecules induced a decrease in cell growth (Figure 6b). The dotted line on the graph represents the level of cell seeding at the beginning of the experiment. At the highest concentration tested (50 μM) 5-FU, the commercial drug, induced a 66% of cell number decrease that is close to maximal complete cell growth inhibition. In this experiment the known derivative 5-FUA (compound **1**) induced only 24% inhibition. In the case of **2** and **3**, they induced a 29 and 44% decrease in cell number, respectively, and are therefore less efficient than the drug 5-FU but more efficient than compound **1**, which is in agreement with the number of units contained in each.

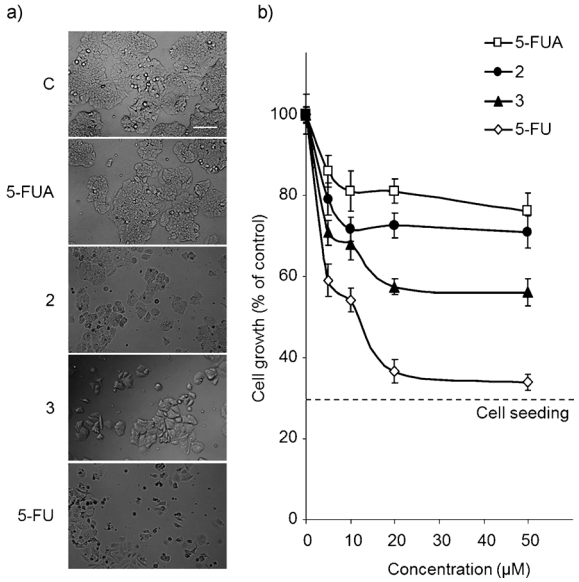

Figure 6. Cytotoxicity of drugs. a) Images of human MCF-7 breast cancer cells incubated for 72 h in the absence (control, C) or presence of the drug (50 μM). The scale bar (top image) represents 30 μm; b) Effect of increasing concentrations (from 5 to 50 μM) of (pro)drugs on MCF-7 cell growth. Values are mean ± SEM of three independent experiments.

Cell-cycle analysis: Since 5-FU is converted in the cell into different cytotoxic metabolites that interfere with DNA synthesis[26] leading to cell cycle arrest and apoptosis, compounds **2** and **3** were studied by using fluorescence-activated cell sorting (FACS) and compared to 5-FU and 5-FUA. In this experiment, MCF-7 cells were treated with 5-FU, 5-FUA, **2** and **3** (50 μM) during 24 h. Figure 7 shows that 5-FU induces cell cycle arrest in the S phase (54 instead of 21% in control cells), an increase in apoptosis (11 instead of 1.5% in control cells) and a total disappearance of G2/M

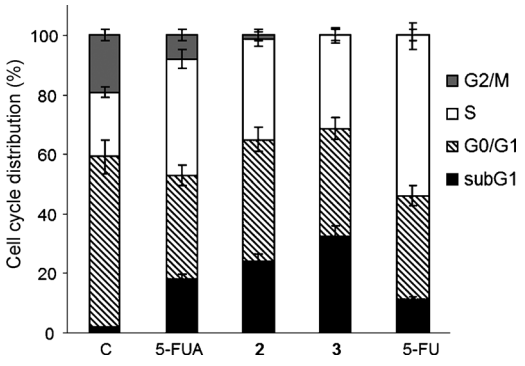

Figure 7. Cell-cycle analysis. MCF-7 cells treated for 24 h with DMSO alone (control, C) or supplemented with 5-FU, 5-FUA, **2**, or **3** (50 μM), respectively.

phase. Whereas cells treated with 5-FUA are arrested in the S phase (43%), a cell population escaped this arrest (9% in G2/M). This could explain, at least in part, the lower efficiency of 5-FUA observed in Figure 6. Concerning compounds **2** and **3**, a significant decrease was noted in the G0/G1 phases (41 and 37%, respectively) in comparison with the control (56%). We can observe the strongest proportion of cells in the apoptotic subG1 phase (24 and 33%, respectively) when treated with **2** and **3**. It is also interesting to note a quasi-total disappearance of G2/M phase in cells treated with **2** and **3**, which is comparable to 5-FU. Finally, these results are in accordance with the cytotoxicity data in Figure 6 demonstrating an efficiency of **2** and **3** between those of 5-FU and 5-FUA.

Synthesis, characterization and studies of materials BS0–BS3: *Blank material **BS0** using only precursor **P1** without drug molecule*: A blank experiment was realized by using only **P1** to give the hybrid material **BS0**, which will serve for comparison. **P1** was dissolved in DMSO and the hydrolysis–condensation was performed with a nucleophilic catalyst (fluoride anion), which leads to a white gel **BS0** after one day. After washing (water, EtOH and acetone successively) and drying (at room temperature) processes, the hybrid was characterized using routine solid-state techniques for analyses.

*Material **BS1** using precursor **P1** and 5-FU*: Subsequently, we considered the synthesis of the corresponding bridged silsesquioxane with 5-FU. In this case, an equimolar amount of **P1** and 5-FU was used and the hydrolysis–condensation was performed under similar reaction conditions as for **BS0** leading to a white gel **BS1** after one day. Figure 8a depicts the solid-state FTIR spectra of 5-FU, **BS0**, and **BS1**, respectively. The IR spectrum of 5-FU shows distinct vibrations between 1700 and 1800 cm^{-1} and unexpectedly, these are not found in the IR spectrum of **BS1**. Instead, vibration bands with similar intensities to those of **BS0** can be seen and both spectra of **BS0** and **BS1** can be completely superimposed (Figure 8a), which suggests that **BS1** like **BS0** is free of 5-FU. This was confirmed by ^{13}C solid-state NMR

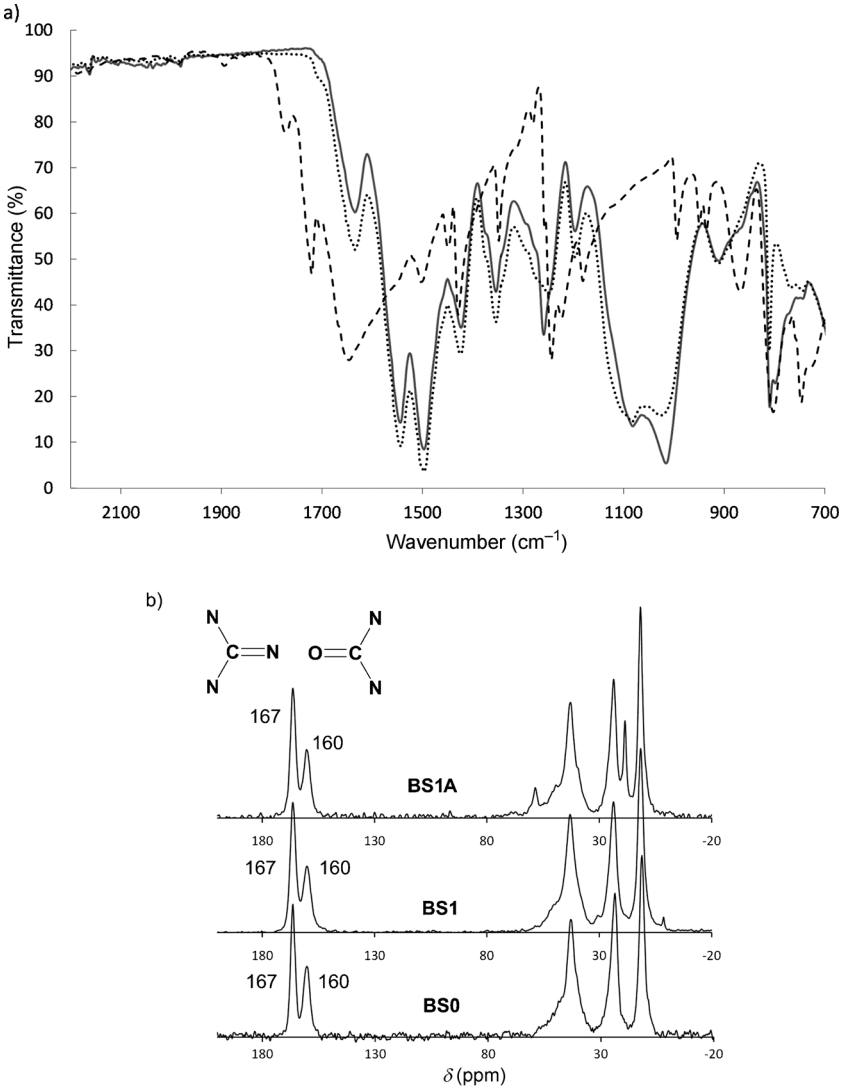

Figure 8. a) FTIR spectra of **BS1** (——), **BS0** (·····), and 5-FU (-----); b) ^{13}C Solid-state NMR spectra of **BS0**, **BS1**, and **BS1A**.

analysis (Figure 8b). Indeed, we compared the ^{13}C NMR spectrum of **BS0** with that of **BS1** and additionally with that of **BS1A** obtained by acid-treatment of **BS1** to deliver any 5-FU that could be present in this hybrid. No typical chemical shifts of 5-FU could be observed in the spectrum of **BS1** and no chemical shift or intensity variation of C=O and C=N peaks was visible between the spectra of **BS0** and **BS1** (Figure 8b).[21] Instead all three spectra could completely be overlapped. In addition, no 5-FU was detected by HPLC in the solution recovered after the acidic treatment and washing of **BS1**. We therefore concluded that the drug molecule, 5-FU, was not retained in the material during the hydrolysis–condensation step. It may be due to the amount of water used, which can cleave the complex during the hybrid preparation and thus explains the release of all 5-FU in solution. Indeed it has already been reported that the H-bonds with 5-FU are sensitive to small molecules such as water and thus appears as an issue to retain it in the resulting BS during the hydrolysis–condensation process.[27] We confirmed this while performing the liquid ^1H NMR spectroscopic investigations with **P1** and 5-FU and showed that the addition of traces of water was sufficient enough to break the H-bonds since the two singlets of N3–H and N1–H completely disappeared (see the Supporting Information S1). This result is different from the one we reported with the cyanuric acid[21] and may be due to the fluorine atom, which weakens the complex. We therefore decided to synthesize two new 5-FU prodrugs (**2** and **3**) with two and three **ADA** patterns, respectively. Compounds **2** and **3** would afford more H-bonding and should induce a stronger complex with **P1** such that they can be maintained in the resulting hybrid materials.

*Material **BS2** and **BS3** using precursor **P1** and **2** and **3***: **BS2** and **BS3** were prepared under the same conditions as above. In these cases, due to the multiple units of 5-FU, ratios of 1:2 and 1:3 were used for **2** and **3**, respectively. In both cases the gels were formed in a much shorter time than for **BS1** (2 h vs. 1 day). This different behavior may result from an easy organization of bridged silsesquioxane due to the existence of the complex. To confirm the presence of 5-FU derivatives in the hybrid materials, FTIR spectroscopy studies were performed.

BS2 behaves similarly to **BS1**, with no retention of **2** despite the presence of two **ADA** patterns most probably because the complex was still not strong enough to resist to several aqueous washings (see the Supporting Information, S2).

Considering **BS3**, interestingly the FTIR spectrum exhibits two characteristic vibration bands (1710 and 1755 cm^{-1}) of **3**, whose intensities remain strictly the same even after washing several times with water (Figure 9). Moreover a broad and intense band appears ranging from 950 to 1100 cm^{-1}, which is attributable to the Si–O–Si vibration, significant of a highly condensed hybrid. In addition, HPLC analysis revealed only traces of **3** in the recovered washing solution from freshly prepared **BS3** showing that the former is well retained in the solid material. Thus, a high loading rate of **3** ($\approx$20 weight %) is expected in **BS3**.

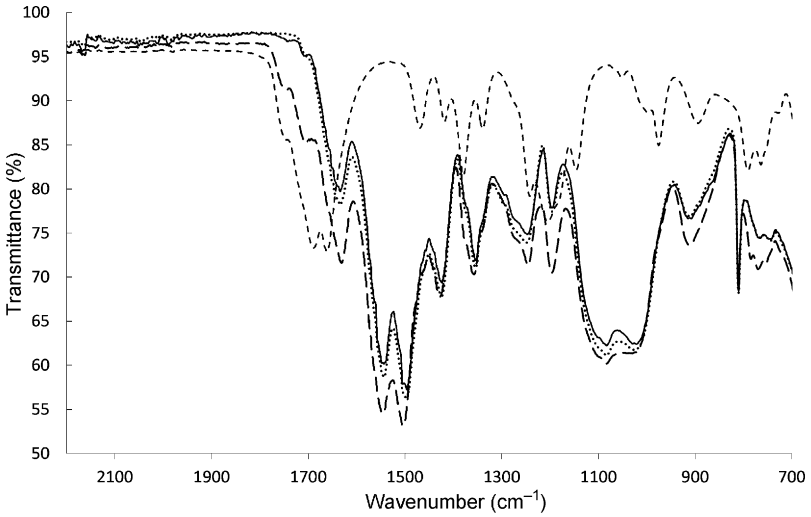

Figure 9. FTIR spectroscopy analysis of **BS3** (– – –), **BS0** (•••••), compound **3** (-----), and **BS3A** (——).

BS3 was then treated with an acid solution (pH 2) leading to **BS3A**. In the corresponding IR spectrum (Figure 9), the two characteristic bands of **3** (1710 and 1755 cm^{-1}) completely disappeared and the liquid ^1H NMR spectrum of the recovered solution confirms the nature of **3**. Moreover, the IR spectra of **BS3A** and **BS0** are identical and can be completely superimposed. All these observations demonstrate the complete elimination of **3** from **BS3** after acid treatment.

The hybrid material **BS3** was also characterized by using usual techniques (see the Supporting Information, S3 and S4). The nitrogen adsorption isotherms of the different materials (**BS3** and **BS3A**) were realized. Essentially weak sorption was observed for both samples meaning that both materials are poorly porous. After the acid treatment of **BS3** to remove **3**, the specific surface did not increase significantly.

As already reported, solid-state ^1H NMR spectroscopy is an appropriate technique to probe the existence of complex through hydrogen bonding.[18a,20] Similarly to the solution ^1H NMR studies on **P1**, it was possible to check the existence of the N3–H bonding of **3** with the silylated triazine fragment in **BS3.** The observations in the solid state were similar to those found in the liquid phase with **P1**. Indeed, the N3–H proton signal at $\delta = 11.1$ ppm of **3** alone nearly disappeared and a weaker band was found downfield at $\delta =$

15.3 ppm for the hybrid **BS3** indicating that the hydrogen-bonding interactions between the anchored triazine derivative and the 5-FU fragments were really preserved in the hybrid material (Figure 10).

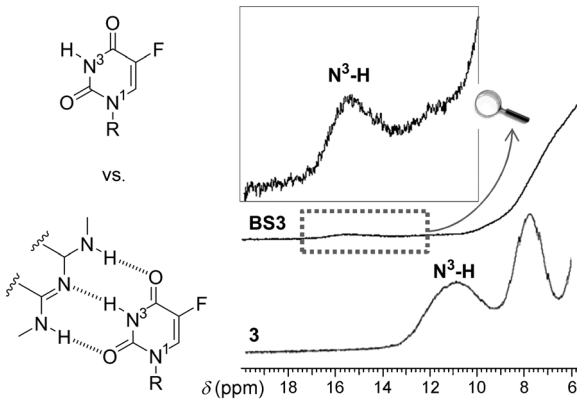

Figure 10. CP-MAS ^{1}H NMR spectra of **BS3** and **3**.

It thus appears clearly that the 9 H-bonds between **P1** and **3** were strong enough to maintain **3** in **BS3** under the sol–gel conditions and during washing process. Treating **BS3** with an acid breaks all the H-bonds to release **3** in solution, which was recovered by filtration and washing of the material. **BS3** is therefore appropriate for an evaluation as a drug carrier.

Prodrug release: For application as a drug-delivery system, the hybrid material should meet moderate pH conditions like those found in lysosomal compartments. We thus envisage three experiments at different pH: pH 7 to confirm that the material meets the zero premature-release criterion, pH 3 to favor a complete release, and pH 5 to mimic the lysosomal pH. The pH-release profile was determined by quantitative HPLC analysis. A suspension of **BS3** was stirred at 37 °C in a phosphate buffer solution (PBS) at the three selected pH (7, 5, and 3). Aliquots of the solution were taken at defined time intervals and replaced by fresh PBS at the same pH to maintain the total volume.

The results are given in Figure 11. The release rate depends directly on the pH value with higher rates at higher concentrations of H^{+} ions as expected. At pH 3, the release is complete after one day, whereas 25 % of **3** were released for endosomal pH 5. After two days at pH 5, the cleavage of **3** occurred inducing wrong HPLC data. Interestingly, in neutral condition no release was observed. These observations confirm that the system bridged silsesquioxane/**3** (**BS3**) can be appropriate as an autonomous drug delivery system with zero premature-release.

Conclusion

In this work, two new 5FU-based prodrugs (**2** and **3**), bearing additional **ADA** patterns (two and three, respectively)

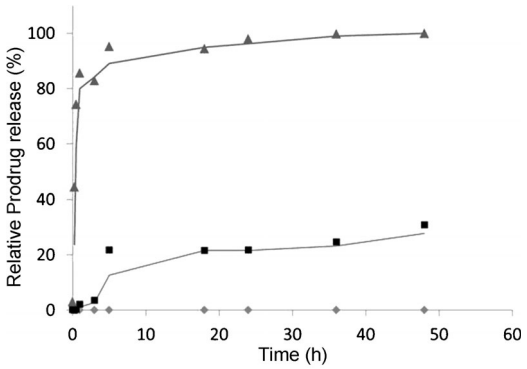

Figure 11. Release of **3** from **BS3** in PBS conditions at different pH values (◆ pH 7, ■ pH 5, ▲ pH 3).

compared with 5-FU have been synthesized. They were all able to form complexes in solution by molecular recognition with a triazine-based organosilane precursor, as demonstrated by liquid ^{1}H NMR studies. Attempts to retain these compounds within the resulting sol–gel-made materials (keeping the **ADA** pattern of the drug linked to the **DAD** pattern of the anchored triazine unit to the silica matrix) to produce pH-responsive bridged silsesquioxanes failed in the case of 5-FU and **2**, but was successful with **3**. This clearly indicates that at least three **ADA** patterns are necessary to strongly hold the prodrug in the BS. Moreover, no release of **3** was observed from the **BS3** at neutral pH but it can be stimulated under mild acid pH. This study demonstrates the interest of developing well-designed bridged silsesquioxanes, despite being non-porous, as new functional hybrid materials for biomedical applications. We envision the use of these BS as carriers for drug-delivery systems since they obviously comply with the required conditions for therapeutic applications, namely a non-premature release (the drug remains in the material under neutral pH) and a controlled-release triggered by an acid stimulus (pH close to weak acidic media of the cell compartments). Work is in progress to synthesize the corresponding nano-BS with the appropriate size to evaluate the acid-triggered self-release of the prodrug inside the cancer cells.

Experimental Section

General: All reactions requiring anhydrous conditions were performed under N_2 atmosphere by using vacuum line and standard Schlenk techniques. Chemicals and solvents were either A.R. grade or purified by standard techniques. Thin layer chromatographies (TLC) were realized with silica gel plates Merck $60F_{254}$ and compounds were visualized under UV light. Column chromatography was performed using flash chromatographer Grace Reveleris, equipped with prepack silica columns (Interchim, 30 μm) with eluent given in parentheses. 5-fluorouracil, chloroacetic acid and 1,1,1-tri(hydroxymethyl)propane, 2,2-dimethylpropane-1,3-diol were purchased from Aldrich, USA. All other solvents and chemicals were obtained from commercial sources.

Compound 1 (5-FUA): Compounds **2** and **3** were synthesized from 5-FUA, which was prepared according to a previously reported method.[23a] Yield: 73 %; m.p. 274–276 °C; ^{1}H NMR (400 MHz, [D_6]DMSO): $\delta = 11.93$

(s, 1H), 8.09 (d, 1H), 4.37 ppm (s, 2H); HRMS (ESI+): calcd for $C_6H_6N_2O_4F$: 189.0312 [$M+H^+$]; found: 189.0313.

Compound 2: Compound **1** (0.5 g, 2.660 mmol) was suspended in freshly distilled $SOCl_2$ (7 mL) at 70 °C under N_2. After 10 h, the excess of $SOCl_2$ was removed under vacuum and the residue was dissolved in dry THF (10 mL). After cooling to 0 °C, 2,2-dimethylpropane-1,3-diol (87.5 mg, 0.841 mmol) was added. The mixture was stirred at room temperature for 10 h and was then filtered on Celite. The solvent was removed under vacuum and the crude product was recrystallized (cyclohexane/dichloromethane: 25:75). Yield: 75%; M.p. decomposition at 180 °C; ^{1}H NMR (400 MHz, [D$_6$]DMSO): δ = 11.99 (s, 2H), 8.07 (d, 2H), 4.50 (s, 4H), 3.92 (s, 4H), 0.88 ppm (s, 6H); ^{13}C NMR (400 MHz, [D$_6$]DMSO): δ = 20.9, 34.7, 48.7, 69.4, 130.4, 138.2, 140.5, 149.6, 157.2, 167.6 ppm; HRMS (ESI+): calcd for $C_{17}H_{19}N_4O_8F_2$; 445.1171 [$M+H^+$]; found: 445.1189.

Compound 3: Compound **1** (0.5 g, 2.660 mmol) was suspended in freshly distilled $SOCl_2$ (7 mL) at 70 °C under N_2. After 10 h, excess of $SOCl_2$ was removed under vacuum and the residue was dissolved in dry THF (10 mL). After cooling to 0 °C, 1,1,1-tri(hydroxymethyl)propane (80 mg, 0.597 mmol) was added. The mixture was stirred at room temperature overnight. The solvent was then removed under vacuum and the residue was purified by column chromatography (dichloromethane/methanol: 98:2→80:20). Yield: 60%; m.p. decomposition after 180 °C; ^{1}H NMR: (400 MHz, [D$_6$]DMSO): δ = 12.03 (s, 3H), 8.03 (d, 3H), 4.49 (s, 6H), 4.04 (s, 6H), 1.36 (q, 2H), 0.79 ppm (t, 3H); ^{13}C NMR (400 MHz, [D$_6$]DMSO): δ = 20.9, 34.7, 48.7, 63.4, 130.1, 138.1, 140.5, 149.6, 157.2, 167.6 ppm; HRMS (ESI+): calcd for $C_{24}H_{24}N_6O_{12}F_3$: 645.1404 [$M+H^+$]; found: 645.1412.

Precursor P1: Compound **P1** was prepared according to a reported procedure.[21] ^{1}H NMR: (400 MHz, $CDCl_3$): δ = 0.58 (t, 4H), 0.91 (t, 6H), 1.18 (t, 18H), 1.54 (m, 8H), 3.06 (q, 4H), 3.27 (m, 4H), 3.41 (m, 4H), 3.60 (m, 4H), 3.78 ppm (q, 12H); ^{13}C NMR (400 MHz, $CDCl_3$): δ = 0.9, 7.5, 11.4, 18.2, 23.0, 23.6, 39.8, 42.5, 42.9, 58.3, 158.8, 165.6 ppm; HRMS (ESI+): calcd for $C_{33}H_{71}N_{10}O_8Si_2$: 791.4995 [$M+H^+$]; found: 791.5006.

Hybrid BS0: Compound **P1** (500 mg, 0.633 mmol) was completely dissolved in DMSO (2 mL) at 50 °C. After 30 min, water (140 μL) and NH_4F (150 μL, 0.25 M solution) were added. A white gel was formed after 1 day and was left under static conditions at room temperature for 3 days. After washing successively with water (50 mL), EtOH (100 mL), and acetone (50 mL), a white powder was obtained and dried under vacuum. ^{29}Si CP-MAS solid-state NMR: δ = −57.5 (T2), −66.5 ppm (T3); ^{13}C CP-MAS solid-state NMR: δ = 11.8, 23.8, 43.4, 160.4, 166.7 ppm.

Hybrid BS1: Compound **P1** (500 mg, 0.633 mmol) and 5-FU (82 mg, 0.631 mmol) were completely dissolved in DMSO (2 mL) at 50 °C. After 30 min, water (140 μL, 7.778 mmol) and NH_4F (150 μL, 0.038 mmol, 0.25 M solution) were added. A white gel was formed after 1 day and was left under static conditions at room temperature for 3 days. After washing successively with water (50 mL), EtOH (100 mL), and acetone (50 mL), **BS1** was obtained as a white powder and dried under vacuum. ^{29}Si CP-MAS solid-state NMR: δ = −57.5 (T2), −66.5 ppm (T3); ^{13}C CP-MAS solid-state NMR: δ = 12.0, 23.8, 43.4, 160.5, 166.9 ppm.

Hybrid BS2: The same procedure was applied to **2** (140 mg, 0.317 mmol), **P1** (500 mg, 0.633 mmol), water (140 μL, 7.778 mmol), DMSO (2 mL) and NH_4F (150 μL, 0.038 mmol, 0.25 M solution). In this case a white gel was formed after 2 h, yielding **BS2** as a white powder.

Hybrid BS3: The same procedure was applied to **3** (136 mg, 0.211 mmol), **P1** (500 mg, 0.633 mmol), water (140 μL, 7.778 mmol), DMSO (2 mL) and NH_4F (150 μL, 0.038 mmol, 0.25 M solution). In this case a white gel was formed after 2 h, yielding **BS3** as a white powder. ^{29}Si CP-MAS solid-state NMR: δ = −57.5 (T2), −66.5 ppm (T3); ^{13}C CP-MAS solid-state NMR: δ = 11.8, 24.0, 43.6, 120–150, 160.1, 166.3 ppm.

Hybrids BS1A–BS3A: Acidic treatments at pH 2 were realized on **BS1–BS3. BS1–BS3** (20 mg) was suspended in ethanol (50 mL) and concentrated HCl (42.5 μL 0.500 mmol) was added. The suspension was stirred at room temperature for 24 h. After filtering and washing with ethanol (20 mL), the solid was suspended in Et_3N (5 mL) and stirred at room temperature for 2 h. The suspension was filtered, washed with ethanol (20 mL) and the hybrid products **BS1A–BS3A** were dried under vacuum.

Characterizations: Discontinuous nitrogen sorption isotherms were measured at 77.15 K using a Micromeritics ASAP 2010. The samples were degassed at 60 °C under vacuum for 12 h before the measurements. The Brunauer–Emmet–Teller (BET) method was used to calculate the specific surface area. Apparatus ESI high-resolution mass spectra (Q-TOF ES+) were obtained by infusing samples into a JEOL MS-DX 300 mass spectrometer. FTIR spectroscopy was carried out using a Perkin–Elmer FTIR system Spectrum BX spectrophotometer. Solid-state NMR spectra were obtained on a Bruker FT-AM 400 spectrometer by using magic-angle spinning mode (MAS) for ^{1}H and CP(cross-polarization)-MAS for ^{13}C and ^{29}Si. Liquid NMR spectra were recorded on a Bruker AC-400 spectrometer. ^{1}H NMR and ^{13}C NMR analysis was performed using $CDCl_3$ or [D$_6$]DMSO as solvent at room temperature. The chemical shifts are expressed in ppm relative to TMS (0 ppm). ^{1}H liquid NMR investigations of the H-bonding were performed in [D$_6$]DMSO with similar concentration of **P1** as used for the hybrids **BS1–3** synthesis. The melting points were determined on Büchi Melting Point B-540 and are uncorrected.

Prodrug release: The release profile was determined by suspending dried samples of the prodrug hybrid carrier (50 mg) in 100 mL of a phosphate buffer solution (PBS) at various pH (pH 7.4, 5, and 3). The solutions were kept at 37 °C with constant stirring at 250 rpm. Aliquots (2 mL) of the samples were taken at defined intervals, and filtered on 0.2 μm PTFE membrane. 2 mL of fresh PBS was added for every aliquot taken at the same pH to maintain the total volume. The release profile was determined by quantitative HPLC on a Shimadzu model LC 20A. The detector wavelength was set at 266 nm. Separation was achieved by isocratic elution with a mobile phase (acetonitrile/ammonium acetate (5 mM aq, 80:20), delivered at a flow-rate of 0.5 mL min^{-1} at ambient temperature through a ZIC-HILIC analytical, MERCK column (150 mm length × 4.6 mm i.d., 5 μm particle size).

Cell culture conditions: Human breast cancer cells (MCF-7) were purchased from ATCC (American Type Culture Collection, Manassas, VA). MCF-7 cells were cultured in DMEM-F12 culture medium supplemented with 10% foetal bovine serum and 50 μg mL^{-1} gentamycin. These cells were allowed to grow in humidified atmosphere at 37 °C under 5% CO_2.

Cytotoxicity evaluation: MCF-7 cells were seeded into 96-well plates at 2×10^4 cells per well in culture medium (200 μL) and allowed to grow for 24 h. Drug and prodrugs were freshly dissolved in DMSO at a concentration of 10^{-2} M and submitted to an ultrasonic bath until complete dissolution. Then, the cells were incubated for 72 h with compounds in a range of concentrations from 5 to 50 μM. Next, a MTT assay was performed to evaluate the toxicity.[28] Briefly, the cells were incubated for 4 h with 0.5 mg mL^{-1} of MTT (3-(4,5-dimethylthiazol-2-yl)-2,5-diphenyltetrazolium bromide; Promega) in media. The MTT/media solution was then removed and the precipitated crystals were dissolved in EtOH/DMSO (1:1). The solution absorbance was read at 540 nm.

Cell-cycle analysis: Flow cytometric analyses were performed on 350000 cells seeded in culture dishes (60 mm diameter) and allowed to grow for 24 h. The cells were then treated with compounds at 50 μM. 24 h after treatment, the cells were harvested and fixed with 70% ethanol overnight. The fixed cells were then incubated with RNase A (1 mg mL^{-1}) and propidium iodide (40 μg mL^{-1}) for 48 h, in the dark at 4 °C. Finally, the DNA content of the cells was analyzed by using a Cytomics FC 500 flow cytometer with CXP software (Beckman Coulter).

Acknowledgements

We are grateful to the CNRS and the French Higher Education and Research Ministry. This work was funded with a young researcher grant from the French National Research agency (ANR-2010-JCJC-1006–01). Montpellier Rio Imaging platform was used for FACS analyses.

[1] a) X. Michalet, F. F. Pinaud, L. A. Bentolila, J. M. Tsay, S. Doose, J. J. Li, G. Sundaresan, A. M. Wu, S. S. Gambhir, S. Weiss, *Science*

2005, *307*, 538–544; b) R. G. Mendes, A. Bachmatiuk, B. Buchner, G. Cuniberti, M. H. Rummeli, *J. Mater. Chem. B* **2013**, *1*, 401–428; c) M. Löbler, K. Sternberg, O. Stachs, R. Allemann, N. Grabow, A. Roock, C. F. Kreiner, D. Streufert, A. T. Neffe, B. D. Hanh, A. Lendlein, K. P. Schmitz, R. Guthoff, *J. Biomed. Mater. Res. Part B* **2011**, *97B*, 388–395; d) M. R. N. Monton, E. M. Forsberg, J. D. Brennan, *Chem. Mater.* **2012**, *24*, 796–811; e) J. Lu, M. Liong, Z. X. Li, J. I. Zink, F. Tamanoi, *Small* **2010**, *6*, 1794–1805; f) Y.-S. Lin, C.-P. Tsai, H.-Y. Huang, C.-T. Kuo, Y. Hung, D.-M. Huang, Y.-C. Chen, C.-Y. Mou, *Chem. Mater.* **2005**, *17*, 4570–4573; g) K. K. Cotí, M. E. Belowich, M. Liong, M. W. Ambrogio, Y. A. Lau, H. A. Khatib, J. I. Zink, N. M. Khashab, J. F. Stoddart, *Nanoscale* **2009**, *1*, 16–39.

[2] a) J. M. Rosenholm, C. Sahlgren, M. Linden, *Nanoscale* **2010**, *2*, 1870–1883; b) B. G. Trewyn, C. M. Whitman, V. S. Y. Lin, *Nano Lett.* **2004**, *4*, 2139–2143; c) J. L. Vivero-Escoto, I. I. Slowing, B. G. Trewyn, V. S. Y. Lin, *Small* **2010**, *6*, 1952–1967; d) B. Munoz, A. Ramila, J. Perez-Pariente, I. Diaz, M. Vallet-Regi, *Chem. Mater.* **2003**, *15*, 500–503; e) P. P. Yang, S. L. Gai, J. Lin, *Chem. Soc. Rev.* **2012**, *41*, 3679–3698; f) M. Gary-Bobo, O. Hocine, D. Brevet, M. Maynadier, L. Raehm, S. Richeter, V. Charasson, B. Loock, A. Morère, P. Maillard, M. Garcia, J.-O. Durand, *Int. J. Pharm.* **2012**, *423*, 509–515.

[3] a) C. Barbé, J. Bartlett, L. Kong, K. Finnie, H. Q. Lin, M. Larkin, S. Calleja, A. Bush, G. Calleja, *Adv. Mater.* **2004**, *16*, 1959–1966; b) D. Avnir, T. Coradin, O. Lev, J. Livage, *J. Mater. Chem.* **2006**, *16*, 1013–1030; c) H. Zhang, D. R. Dunphy, X. Jiang, H. Meng, B. Sun, D. Tarn, M. Xue, X. Wang, S. Lin, Z. Ji, R. Li, F. L. Garcia, J. Yang, M. L. Kirk, T. Xia, J. I. Zink, A. Nel, C. J. Brinker, *J. Am. Chem. Soc.* **2012**, *134*, 15790–15804.

[4] a) M. W. Ambrogio, C. R. Thomas, Y.-L. Zhao, J. I. Zink, J. F. Stoddart, *Acc. Chem. Res.* **2011**, *44*, 903–913; b) Z. X. Li, J. L. Nyalosaso, A. A. Hwang, D. P. Ferris, S. Yang, G. Derrien, C. Charnay, J. O. Durand, J. I. Zink, *J. Phys. Chem. C* **2011**, *115*, 19496–19506; c) J. Lu, E. Choi, F. Tamanoi, J. I. Zink, *Small* **2008**, *4*, 421–426; d) D. P. Ferris, J. Lu, C. Gothard, R. Yanes, C. R. Thomas, J. C. Olsen, J. F. Stoddart, F. Tamanoi, J. I. Zink, *Small* **2011**, *7*, 1816–1826; e) D. L. Clemens, B. Y. Lee, M. Xue, C. R. Thomas, H. Meng, D. Ferris, A. E. Nel, J. I. Zink, M. A. Horwitz, *Antimicrob. Agents Chemother.* **2012**, *56*, 2535–2545.

[5] a) C. H. Lee, S. H. Cheng, I. P. Huang, J. S. Souris, C. S. Yang, C. Y. Mou, L. W. Lo, *Angew. Chem.* **2010**, *122*, 8390–8395; *Angew. Chem. Int. Ed.* **2010**, *49*, 8214–8219; b) Z. Luo, K. Y. Cai, Y. Hu, L. Zhao, P. Liu, L. Duan, W. H. Yang, *Angew. Chem.* **2011**, *123*, 666–669; *Angew. Chem. Int. Ed.* **2011**, *50*, 640–643; c) A. Baeza, E. Guisasola, E. Ruiz-Hernandez, M. Vallet-Regi, *Chem. Mater.* **2012**, *24*, 517–524.

[6] a) K. J. Shea, D. A. Loy, O. W. Webster, *Chem. Mater.* **1989**, *1*, 572–574; b) R. J. P. Corriu, J. J. E. Moreau, P. Thépot, M. Wong Chi Man, *Chem. Mater.* **1992**, *4*, 1217–1224.

[7] a) C. Sanchez, F. Ribot, *New J. Chem.* **1994**, *18*, 1007–1047; b) K. J. Shea, J. J. E. Moreau, D. A. Loy, R. J. P. Corriu, B. Boury in *Functional Hybrid Materials* (Eds.: P. Gomez-Romero, C. Sanchez), Wiley-VCH, Weinheim, **2004**, pp. 50–85.

[8] a) X. Elias, R. Pleixats, M. Wong Chi Man, J. J. E. Moreau, *Adv. Synth. Catal.* **2006**, *348*, 751–762; b) A. Zamboulis, N. Moitra, J. J. E. Moreau, X. Cattoën, M. Wong Chi Man, *J. Mater. Chem.* **2010**, *20*, 9322–9338; c) A. Monge-Marcet, R. Pleixats, X. Cattoën, M. Wong Chi Man, *Catal. Sci. Technol.* **2011**, *1*, 1544–1563.

[9] a) J. Graffion, X. Cattoën, V. Freitas, R. A. S. Ferreira, M. Wong Chi Man, L. D. Carlos, *J. Mater. Chem.* **2012**, *22*, 6711–6715; b) J. Graffion, X. Cattoën, M. Wong Chi Man, V. R. Fernandes, P. S. André, R. A. S. Ferreira, L. D. Carlos, *Chem. Mater.* **2011**, *23*, 4773–4782.

[10] S. Bourg, J. C. Broudic, O. Conocar, J. J. E. Moreau, D. Meyer, M. Wong Chi Man, *Chem. Mater.* **2001**, *13*, 491–499.

[11] a) P. Chevalier, R. J. P. Corriu, P. Delord, J. J. E. Moreau, M. Wong Chi Man, *New J. Chem.* **1998**, *22*, 423–433; b) P. M. Chevalier, R. J. P. Corriu, J. J. E. Moreau, M. Wong Chi Man, *J. Sol-Gel Sci. Technol.* **1997**, *8*, 603–607.

[12] a) T. Asefa, M. J. MacLachlan, N. Coombs, G. A. Ozin, *Nature* **1999**, *402*, 867–871; b) S. Inagaki, S. Guan, Y. Fukushima, T. Ohsuna, O. Terasaki, *J. Am. Chem. Soc.* **1999**, *121*, 9611–9614.

[13] S. Inagaki, S. Guan, T. Ohsuna, O. Terasaki, *Nature* **2002**, *416*, 304–307.

[14] P. Van Der Voort, D. Esquivel, E. De Canck, F. Goethals, I. Van Driessche, F. J. Romero-Salguero, *Chem. Soc. Rev.* **2013**, *42*, 3913.

[15] a) C. X. Lin, S. Z. Qiao, C. Z. Yu, S. Ismadji, G. Q. Lu, *Microporous Mesoporous Mater.* **2009**, *117*, 213–219; b) R. Vathyam, E. Wondimu, S. Das, C. Zhang, S. Hayes, Z. Tao, T. Asefa, *J. Phys. Chem. C* **2011**, *115*, 13135–13150; c) M. S. Moorthy, S. S. Park, D. Fuping, S. H. Hong, M. Selvaraj, C. S. Ha, *J. Mater. Chem.* **2012**, *22*, 9100–9108.

[16] N. Mizoshita, T. Tani, H. Shinokubo, S. Inagaki, *Angew. Chem.* **2012**, *124*, 1182–1186; *Angew. Chem. Int. Ed.* **2012**, *51*, 1156–1160.

[17] a) J. J. E. Moreau, B. P. Pichon, G. Arrachart, M. Wong Chi Man, C. Bied, *New J. Chem.* **2005**, *29*, 653–658; b) G. Arrachart, A. Bendjerriou, C. Carcel, J. J. E. Moreau, M. Wong Chi Man, *New J. Chem.* **2010**, *34*, 1436–1440.

[18] a) G. Arrachart, C. Carcel, J. J. E. Moreau, G. Hartmeyer, B. Alonso, D. Massiot, G. Creff, J. L. Bantignies, P. Dieudonné, M. Wong Chi Man, G. Althoff, F. Babonneau, C. Bonhomme, *J. Mater. Chem.* **2008**, *18*, 392–399; b) M. Wong Chi Man, G. Arrachart, C. Carcel, J. J. E. Moreau, C. Bonhomme, F. Babonneau, G. Creff, J. L. Bantignies, P. Dieudonné, B. Alonso, *Org./Inorg. Hybrid Mater.* **2008**, *1007*, 3–14.

[19] G. Arrachart, G. Creff, H. Wadepohl, C. Blanc, C. Bonhomme, F. Babonneau, B. Alonso, J. L. Bantignies, C. Carcel, J. J. E. Moreau, P. Dieudonné, J. L. Sauvajol, D. Massiot, M. Wong Chi Man, *Chem. Eur. J.* **2009**, *15*, 5002–5005.

[20] G. Arrachart, C. Carcel, P. Trens, J. J. E. Moreau, M. Wong Chi Man, *Chem. Eur. J.* **2009**, *15*, 6279–6288.

[21] L. Fertier, C. Théron, C. Carcel, P. Trens, M. Wong Chi Man, *Chem. Mater.* **2011**, *23*, 2100–2106.

[22] E. S. Lee, K. T. Oh, D. Kim, Y. S. Youn, Y. H. Bae, *J. Controlled Release* **2007**, *123*, 19–26.

[23] a) Q. Luo, P. Wang, Y. Miao, H. He, X. Tang, *Carbohydr. Polym.* **2012**, *87*, 2642–2647; b) C. Sang Mok Chung, Y. Eun Jeong, K. So Hee, L. Myung Gull, L. Heejoo, P. Man Ki, K. Chong-Kook, *Int. J. Pharm.* **1991**, *68*, 61–68.

[24] J. Xiong, H.-F. Zhu, Y.-J. Zhao, Y.-J. Lan, J.-W. Jiang, J.-J. Yang, S.-F. Zhang, *Molecules* **2009**, *14*, 3142–3152.

[25] D.-W. Li, F.-F. Tian, Y.-S. Ge, X.-L. Ding, J.-H. Li, Z.-Q. Xu, M.-F. Zhang, X.-L. Han, R. Li, F.-L. Jiang, Y. Liu, *Chem. Commun.* **2011**, *47*, 10713–10715.

[26] R. Yoshikawa, M. Kusunoki, H. Yanagi, M. Noda, J.-i. Furuyama, T. Yamamura, T. Hashimoto-Tamaoki, *Cancer Res.* **2001**, *61*, 1029–1037.

[27] Z. Zhou, D. Bong, *Langmuir* **2013**, *29*, 144–150.

[28] M. Maynadier, J.-M. Ramirez, A.-M. Cathiard, N. Platet, D. Gras, M. Gleizes, M. S. Sheikh, P. Nirde, M. Garcia, *FASEB J.* **2007**, *22*, 671–681.

Received: March 20, 2013
Published online: August 8, 2013

